

Next-to-next-to-leading-order QCD corrections to $\chi_{c0,2} \rightarrow \gamma\gamma$

Wen-Long Sang,^{1,2} Feng Feng,³ Yu Jia,^{4,5} and Shuang-Ran Liang⁴

¹*School of Physical Science and Technology, Southwest University, Chongqing 400700, China*

²*State Key Laboratory of Theoretical Physics, Institute of Theoretical Physics, Chinese Academy of Sciences, Beijing 100190, China*

³*China University of Mining and Technology, Beijing 100083, China*

⁴*Institute of High Energy Physics and Theoretical Physics Center for Science Facilities, Chinese Academy of Sciences, Beijing 100049, China*

⁵*Center for High Energy Physics, Peking University, Beijing 100871, China*

(Dated: December 23, 2015)

We calculate the next-to-next-to-leading-order (NNLO) perturbative corrections to P -wave quarkonia annihilation decay to two photons, in the framework of nonrelativistic QCD (NRQCD) factorization. The order- α_s^2 short-distance coefficients associated with each helicity amplitude are presented in a semi-analytic form, including the “light-by-light” contributions. With substantial NNLO corrections, we find disquieting discrepancy when confronting our state-of-the-art predictions with the latest BESIII measurements, especially fail to account for the measured $\chi_{c2} \rightarrow \gamma\gamma$ width. Incorporating the effects of spin-dependent forces would even exacerbate the situation, since it lifts the degeneracy between the nonperturbative NRQCD matrix elements of χ_{c0} and χ_{c2} toward the wrong direction. We also present the order- α_s^2 predictions to $\chi_{b0,2} \rightarrow \gamma\gamma$, which await the future experimental test.

PACS numbers: 12.38.Bx, 13.20.Gd, 14.40.Pq

Charmonium decay has historically played an important role in establishing the asymptotic freedom of QCD, and served as a clean platform to probe the interplay between perturbative and nonperturbative dynamics [1, 2]. Among them, the electromagnetic decay $\chi_{c0,2} \rightarrow \gamma\gamma$ provide a particularly interesting, and, rich testing ground of QCD [3, 4]. In the past decades, these decay channels have been extensively studied from various theoretical angles, such as nonrelativistic potential model [5, 6], relativistic quark model [7–9], Bethe-Salpeter approach [10], nonrelativistic QCD (NRQCD) factorization [11, 12], as well as lattice QCD [13]. On the experimental side, they were previously measured by CLEO-c [14]. BESIII experiment [15] has recently reported their high precision results,

$$\Gamma_{\gamma\gamma}(\chi_{c0}) = (2.33 \pm 0.20 \pm 0.13 \pm 0.17) \text{ keV}, \quad (1a)$$

$$\Gamma_{\gamma\gamma}(\chi_{c2}) = (0.63 \pm 0.04 \pm 0.04 \pm 0.04) \text{ keV}. \quad (1b)$$

In addition, BESIII presents the ratio of the decay rates between χ_{c2} and χ_{c0} . For the first time, they also measured the ratio of the two polarized decay rates for χ_{c2} :

$$\mathcal{R} = \frac{\Gamma_{\gamma\gamma}(\chi_{c2})}{\Gamma_{\gamma\gamma}(\chi_{c0})} = 0.271 \pm 0.029 \pm 0.013 \pm 0.027, \quad (2a)$$

$$f_{0/2} = \frac{\Gamma_{\gamma\gamma}^{\lambda=0}(\chi_{c2})}{\Gamma_{\gamma\gamma}^{\lambda=2}(\chi_{c2})} = 0.00 \pm 0.02 \pm 0.02, \quad (2b)$$

where $\lambda = |\lambda_1 - \lambda_2|$, and $\lambda_1, \lambda_2 = \pm 1$ denote the helicities

of the outgoing photons. The precise data thereby calls for the full-fledged theoretical inspection.

In parallel with positronium decay, the leading-order NRQCD prediction to $\chi_{c0,2} \rightarrow \gamma\gamma$ in the nonrelativistic limit is extremely simple, yields $\mathcal{R} = 4/15 \approx 0.27$ [16]. This is impressively consistent with the measurement (2a). Nevertheless, these processes are sensitive to the next-to-leading-order (NLO) radiative correction [17, 18], with the predicted \mathcal{R} scattered in the range from 0.09 to 0.36 [6, 7].

To date, the next-to-next-to-leading-order (NNLO) radiative corrections are only available for a few S -wave quarkonium electromagnetic decay processes, exemplified by $\Upsilon(J/\psi) \rightarrow e^+e^-$ [19, 20], $\eta_{b,c} \rightarrow \gamma\gamma$ [21, 22], and $B_c \rightarrow \ell\nu$ [23, 24], as well as the $\gamma\gamma^* \rightarrow \eta_{c,b}$ transition form factor [22]. It has been found that the NNLO radiative corrections in aforementioned processes are often negative and substantial. The goal of this work is to address the complete NNLO corrections to P -wave quarkonium annihilation into two photons.

The partial widths for $\chi_{c0,2} \rightarrow \gamma\gamma$ can be expressed as

$$\Gamma_{\gamma\gamma}(\chi_0) = \frac{1}{16\pi} \left(2|\mathcal{A}_{1,1}^{\chi_0}|^2 \right), \quad (3a)$$

$$\Gamma_{\gamma\gamma}(\chi_2) = \frac{1}{5} \frac{1}{16\pi} \left(2|\mathcal{A}_{1,1}^{\chi_2}|^2 + 2|\mathcal{A}_{1,-1}^{\chi_2}|^2 \right), \quad (3b)$$

where $\mathcal{A}_{\lambda_1, \lambda_2}^{\chi_J}$ signifies the helicity amplitude for $\chi_{cJ} \rightarrow$

$\gamma(\lambda_1)\gamma(\lambda_2)$. We have employed parity invariance to only enumerate the independent helicity amplitudes in (3).

NRQCD factorization approach, which exploits the nonrelativistic nature of heavy quarkonium, provides a systematic and model-independent framework to tackle quarkonium decay [11]. At the lowest order in v , the helicity amplitudes in (3) can be written in a factorized form:

$$\mathcal{A}_{\lambda_1, \lambda_2}^{\chi_{0,2}} = \mathcal{C}_{\lambda}^{\chi_{0,2}}(m, \mu_R, \mu_{\Lambda}) \frac{\langle 0 | \chi^\dagger \mathcal{K}_{3P_{0,2}} \psi(\mu_{\Lambda}) | \chi_{c0,2} \rangle}{m^{3/2}} + \mathcal{O}(v^2), \quad (4)$$

where

$$\mathcal{K}_{3P_0} = \frac{1}{\sqrt{3}}(-\frac{i}{2} \vec{\mathbf{D}} \cdot \boldsymbol{\sigma}), \quad (5a)$$

$$\mathcal{K}_{3P_2} = -\frac{i}{2} \vec{\mathbf{D}}^{(i} \sigma^j) \epsilon^{*ij}, \quad (5b)$$

with ϵ^{ij} representing the polarization tensor of χ_{c2} .

$\mathcal{C}_{\lambda}^{\chi_{0,2}}(m, \mu_R, \mu_{\Lambda})$ in (4) signifies the NRQCD short-distance coefficient (SDC), where m , μ_R , μ_{Λ} denote the charm quark mass, renormalization scale, and NRQCD factorization scale, respectively. In phenomenological analysis, these nonperturbative matrix elements are often substituted as the derivative of P -wave radial Schrödinger wave functions at the origin:

$$\langle 0 | \chi^\dagger \mathcal{K}_{3P_{0,2}} \psi(\mu_{\Lambda}) | \chi_{c0,2} \rangle = \sqrt{\frac{3N_c}{2\pi}} \overline{R'}_{\chi_{c0,2}}(\mu_{\Lambda}), \quad (6)$$

where $N_c = 3$ is the number of color. In literature, it is often assumed that $\overline{R'}_{\chi_{c0}} \approx \overline{R'}_{\chi_{c2}}$ by invoking the approximate heavy quark spin symmetry (HQSS). We stress that, in NRQCD these wave functions at the origin are promoted as scale-dependent quantities.

Thanks to the asymptotic freedom, the SDCs can be computed order by order in α_s . Through NNLO in α_s , the SDC affiliated with the only helicity channel of χ_{c0} is

$$\mathcal{C}_0^{\chi_0} = \frac{4\sqrt{3}\pi e_Q^2 \alpha}{\sqrt{m}} \left\{ 1 + C_F \frac{\alpha_s(\mu_R)}{\pi} \left(\frac{\pi^2}{8} - \frac{7}{6} \right) + \frac{\alpha_s^2}{\pi^2} \left[C_F \frac{\beta_0}{4} \left(\frac{\pi^2}{8} - \frac{7}{6} \right) \ln \frac{\mu_R^2}{m^2} + \Delta_0^{\chi_0} \right] \right\}, \quad (7)$$

and two independent SDCs $\mathcal{C}_{0,2}^{\chi_2}$ are

$$\mathcal{C}_0^{\chi_2} = \frac{4\sqrt{6}\pi \alpha e_Q^2}{3\sqrt{m}} \left\{ C_F \frac{\alpha_s(\mu_R)}{\pi} \left(\frac{3\pi^2}{8} - 6 \ln 2 + 1 \right) + \frac{\alpha_s^2}{\pi^2} \left[C_F \frac{\beta_0}{4} \left(\frac{3\pi^2}{8} - 6 \ln 2 + 1 \right) \ln \frac{\mu_R^2}{m^2} + \Delta_0^{\chi_2} \right] \right\}, \quad (8a)$$

$$\mathcal{C}_2^{\chi_2} = -\frac{8\pi \alpha e_Q^2}{\sqrt{m}} \left\{ 1 - 2C_F \frac{\alpha_s(\mu_R)}{\pi} + \frac{\alpha_s^2}{\pi^2} \left(-2C_F \frac{\beta_0}{4} \ln \frac{\mu_R^2}{m^2} + \Delta_2^{\chi_2} \right) \right\}. \quad (8b)$$

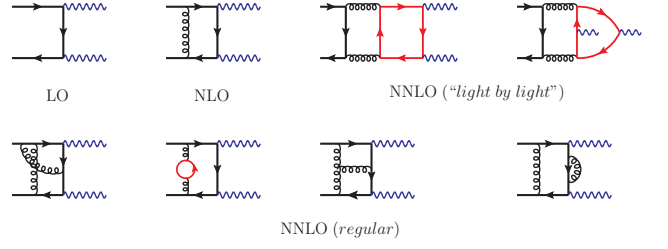


FIG. 1: Representative Feynman diagrams for $c\bar{c}({}^3P_J^{(1)}) \rightarrow \gamma\gamma$ through order α_s^2 .

$\beta_0 = \frac{11}{3}C_A - \frac{2}{3}(n_L + n_H)$ is the one-loop coefficient of the QCD β -function, where $n_H = 1$, and n_L signifies the number of light quark flavors ($n_L = 3$ for χ_c , 4 for χ_b). The occurrence of the $\beta_0 \ln \mu_R$ term in (7) and (8) is demanded by renormalization group invariance.

To the best of our knowledge, the NLO perturbative correction to the $\lambda = 0$ amplitude in (8a) is new. Interestingly, this helicity amplitude turns out to vanish at Born level. Thus, NRQCD framework appears to offer a natural explanation for the tiny value of $f_{0/2}$ in (2b) observed by BESIII.

The nontrivial task is then to decipher $\Delta_{0,2}^{\chi_{0,2}}$.

Rather than follow the literal matching doctrine, we employ the standard shortcut of directly extracting the SDCs [19, 20]. We compute the on-shell quark amplitude for $c\bar{c}({}^3P_J^{(1)}) \rightarrow \gamma\gamma$ through order α_s^2 . In contrast to the S -wave quarkonium decay, we expand the corresponding amplitude to the first order in q , the relative momentum between c and \bar{c} , to identify the P -wave component, and compose the $c\bar{c}({}^3P_{0,2}^{(1)})$ state via the standard procedure [12]. In the end we project out the respective helicity amplitudes. A key simplification originates from the fact that, when conducting the loop integration, q has already been set to zero.

We briefly describe the calculation. The package *FeynArts* [25] is employed to generate corresponding Feynman diagrams and amplitudes through $\mathcal{O}(\alpha_s^2)$ in Feynman gauge. There are 108 regular 2-loop diagrams and 12 “light-by-light” (LBL) scattering diagrams, some of which are sketched in Fig. 1. The latter gauge-invariant subsets are UV- and IR-finite. Dimensional regularization (DR) is employed to regularize both UV and IR divergences. We then use *FeynCalc/FormLink* [26, 27] to carry out the trace over Dirac/color matrices. The packages *Apart* [28] and *FIRE* [29] are utilized to conduct partial fraction together with integration-by-parts (IBP) reduction. Finally, we end up with around 80 master integrals (MI). For a dozen of simpler MIs, we employ the α parameters [30] as well as the Mellin-Barnes tools *AMBRE* [31]/*MB* [32] to infer the (semi-) analytic expressions; for the multi-leg two-loop MIs, we combine *FIESTA/CubPack* [33, 34] to carry out sector decomposition and subsequent numerical integrations with quadru-

ple precision.

The order- α_s^2 expressions for the heavy quark wave function and mass renormalization constants are taken from [35, 36]. The strong coupling constant is renormalized to one-loop order under $\overline{\text{MS}}$ scheme. All the UV divergences are eliminated by the renormalization procedure. However, at this stage, the NNLO amplitudes still contain single IR poles, with coefficients differing from the 3P_0 to the 3P_2 channel.

These single IR poles are intimately connected to the anomalous dimensions of the NRQCD color-singlet currents associated with $^3P_{0,2}$, as specified in (5). In fact, from the lower-energy effective field theory of NRQCD, Hoang and Ruiz-Femenia are able to predict the anomalous dimensions for NRQCD bilinear carrying general $^{2S+1}L_J$ quantum number [37]. Particularly, the anomalous dimensions of the operators carrying quantum number 3P_J are predicted to be

$$\gamma_{^3P_0} = -C_F \left(\frac{C_F}{6} + \frac{C_A}{24} \right) \alpha_s^2 + \mathcal{O}(\alpha_s^3), \quad (9a)$$

$$\gamma_{^3P_2} = -C_F \left(\frac{13C_F}{240} + \frac{C_A}{24} \right) \alpha_s^2 + \mathcal{O}(\alpha_s^3). \quad (9b)$$

Their difference signals the violation of HQSS due to spin-dependent interactions.

It is reassuring that the coefficients of the uncanceled IR poles in our NNLO amplitudes turn out to exactly match the UV poles as implied in (9). In our opinion, this is a highly nontrivial verification of the correctness of our calculation.

We thereby factorize these IR poles into the corresponding $\chi_{c0,2}$ -to-vacuum NRQCD matrix elements in (4) under $\overline{\text{MS}}$ prescription, with $\ln \mu_\Lambda$ now manifested in the respective SDCs.

The $\Delta_\lambda^{\chi_J}$ receives contributions from both regular and LBL diagrams, where the former is real valued, and the latter complex valued. It is convenient to decompose $\Delta_\lambda^{\chi_J}$ into two parts:

$$\Delta_\lambda^{\chi_J} = \Delta_{\text{reg}, \lambda}^{\chi_J} + \Delta_{\text{lbl}, \lambda}^{\chi_J}. \quad (10)$$

The regular part can be organized according to their color structure:

$$\begin{aligned} \Delta_{\text{reg}, \lambda}^{\chi_J} = & C_F^2 s_{A;\lambda}^{\chi_J} + C_F C_A s_{NA,\lambda}^{\chi_J} + n_L C_F T_F s_{L,\lambda}^{\chi_J} \\ & + n_H C_F T_F s_{H,\lambda}^{\chi_J}, \end{aligned} \quad (11)$$

where $C_F = \frac{4}{3}$, $C_A = 3$, $T_F = \frac{1}{2}$ are $SU(3)$ color factors.

The regular pieces of the only helicity component for

χ_0 are

$$\begin{aligned} s_{A,0}^{\chi_0} &= -\frac{2\pi^2}{3} \ln \frac{\mu_\Lambda}{m} - 9.14751077(6), \\ s_{NA,0}^{\chi_0} &= -\frac{\pi^2}{6} \ln \frac{\mu_\Lambda}{m} - 1.69821088(5), \\ s_{L,0}^{\chi_0} &= \frac{1}{432} \left[-126\zeta(3) - 45\pi^2 + 244 \right], \\ s_{H,0}^{\chi_0} &= 0.09292479(2). \end{aligned} \quad (12)$$

The regular pieces affiliated with the two helicity components of χ_2 are

$$\begin{aligned} s_{A,0}^{\chi_2} &= -1.59023228(9), \\ s_{NA,0}^{\chi_2} &= 2.13274690(5), \\ s_{L,0}^{\chi_2} &= -\frac{7}{8}\zeta(3) - \frac{3\pi^2}{16} - 2\ln^2 2 + \frac{16}{3}\ln 2 - \frac{5}{9}, \\ s_{H,0}^{\chi_2} &= 0.01594186(1), \end{aligned} \quad (13)$$

and

$$\begin{aligned} s_{A,2}^{\chi_2} &= -\frac{13\pi^2}{60} \ln \frac{\mu_\Lambda}{m} - 5.93023533(7), \\ s_{NA,2}^{\chi_2} &= -\frac{\pi^2}{6} \ln \frac{\mu_\Lambda}{m} - 5.78204922(4), \\ s_{L,2}^{\chi_2} &= \frac{43}{36} + \frac{\pi^2}{16}, \\ s_{H,2}^{\chi_2} &= 0.021716502(9). \end{aligned} \quad (14)$$

Note that the absence of $\ln \mu_\Lambda$ in (13) originates from the vanishing of LO amplitude for the helicity configuration $\chi_2 \rightarrow \gamma(\pm 1)\gamma(\pm 1)$.

In contrast to regular part, it is rather challenging for FIESTA to acquire high-precision results for the complex-valued MIs associated with the LBL diagrams. Fortunately, some of them can be worked out analytically. Employing the α -parameters [30] or Mellin-Barnes tools [31, 32], it is always feasible to reduce the remaining MIs into one or two-dimensional integrals, which can then be readily computed with high numerical precision.

The LBL part for the $\chi_0 \rightarrow \gamma(\pm 1)\gamma(\pm 1)$ is

$$\begin{aligned} \Delta_{\text{lbl},0}^{\chi_0} = & (-0.120326 + 0.398547i)n_H C_F T_F \\ & + \left(0.953741 + \frac{i\pi}{6} \right) C_F T_F \sum_i^{n_L} \frac{e_i^2}{e_Q^2}, \end{aligned} \quad (15)$$

where e_i represents the electric charge of the i -th light flavor.

The LBL pieces associated with the two helicity com-

ponents of χ_2 are

$$\Delta_{\text{lbl},0}^{\chi_2} = \left(-0.019772 + 0.011196i \right) n_H C_F T_F + \left[0.359850 + i\pi \left(\frac{7\pi^2}{6} - \frac{23}{2} \right) \right] C_F T_F \sum_i^{n_L} \frac{e_i^2}{e_Q^2}, \quad (16a)$$

$$\Delta_{\text{lbl},2}^{\chi_2} = \left(-0.088227 + 0.187239i \right) n_H C_F T_F + \left[-0.669873 + \frac{\pi}{27}(91 - 12\pi^2 + 24 \ln 2)i \right] \times C_F T_F \sum_i^{n_L} \frac{e_i^2}{e_Q^2}. \quad (16b)$$

In passing, we recall that the rare decay process $\chi_{c2} \rightarrow e^+e^-$ contains uncanceled IR divergences [38]. Since the occurring one-loop box diagrams just comprise subdiagrams of our two-loop LBL diagrams, it is intriguing that our LBL contributions turn out to be completely IR finite.

With all the order- α_s^2 terms in (10) available in a semi-analytic form, we can assemble them together to deduce the corresponding SDCs in (7), (8), and substitute them into (4) to deduce the respective helicity amplitudes, finally obtain the desired two-photon widths for $\chi_{c0,2}$ according to (3).

First we would like to predict $f_{0/2}$ and \mathcal{R} and compare with BESIII experiments. Following the analysis conducted for the ratio of the decay rates of $J/\psi \rightarrow e^+e^-$ to $\eta_c \rightarrow \gamma\gamma$ [21, 39], we also expand these two ratios strictly to the second order in α_s :

$$\mathcal{R} = \frac{4}{15}\Omega \left[1 - \left(\frac{\pi^2}{3} + \frac{20}{9} \right) \frac{\alpha_s}{\pi} - \left(5.855 + 22.967 \ln \frac{\mu_R}{m} + 15.791 \ln \frac{m}{\mu_\Lambda} \right) \left(\frac{\alpha_s}{\pi} \right)^2 \right], \quad (17a)$$

$$f_{0/2} = \frac{\alpha_s^2}{216\pi^2} (8 + 3\pi^2 - 48 \ln 2)^2, \quad (17b)$$

where $n_L = 3$ has been taken, and Ω is defined by

$$\Omega = \left| \frac{\overline{R'_{\chi_{c2}}}(\mu_\Lambda)}{\overline{R'_{\chi_{c0}}}(\mu_\Lambda)} \right|^2, \quad (18)$$

which characterizes the extent of the violation of HQSS.

With the nonperturbative matrix elements cancelled, the helicity ratio $f_{0/2}$ is entirely determined by the order- α_s (leading) contribution of the $\lambda = 0$ component from χ_2 decay in (8a).

In the following phenomenological analysis, we will use the two-loop quark pole masses as $m_c = 1.68$ GeV and $m_b = 4.78$ GeV [22]. Running strong coupling at a given scale is evaluated by the package RunDec [40].

We first present the NRQCD predictions accurate to NLO in α_s :

$$\mathcal{R} = (0.124_{-0.028}^{+0.032}) \Omega, \quad f_{0/2} = 0, \quad (19)$$

	μ_Λ	LO	NLO	NNLO
χ_{c0}	1 GeV	0.032 ± 0.004	0.036 ± 0.005	$0.091_{-0.024}^{+0.087}$
	m			$0.127_{-0.049}^{+8.598}$
χ_{c2}	1 GeV	0.032 ± 0.004	$0.076_{-0.021}^{+0.031}$	—
	m			—

TABLE I: Determination of $|\overline{R'_{\chi_{cJ}}}(\mu_\Lambda)|^2$ (GeV⁵) from BESIII data at various level of perturbative accuracy. The uncertainty is estimated by combining the experimental error with that by varying μ_R from 1 GeV to $2m$.

where the uncertainty comes from varying the renormalization scale in the range $1 \text{ GeV} < \mu_R < 2m$, with central value at $\mu_R = m$. Assuming $\Omega = 1$, the predicted \mathcal{R} then becomes considerably smaller than the BESIII data in (2a).

From (17), we further give our predictions at NNLO accuracy:

$$\mathcal{R} = (0.075_{-0.051}^{+0.044}) \Omega, \quad f_{0/2} = 0.0009_{-0.0004}^{+0.0009}, \quad (20)$$

with the central values obtained by setting $\mu_\Lambda = 1 \text{ GeV}$ and $\mu_R = m$. Two kinds of uncertainties are included by sliding the μ_Λ, μ_R in the range $\frac{m}{2} < \mu_\Lambda < m$ and $1 \text{ GeV} < \mu_R < 2m$, respectively.

While the very tiny $f_{0/2}$ predicted in (20) fully agrees with the BESIII measurement within errors, the NNLO prediction of \mathcal{R} deviates further from the data relative to the NLO prediction, in the HQSS limit.

If the HQSS-violating effects would lead to $\Omega > 1$, our NNLO predictions in (20) would still have chance to agree with the data. The spin-dependent interactions such as spin-orbital force and tensor force have been incorporated to study the fine splitting among χ_{cJ} [41]. In order to elucidate the role played by the HQSS violation, we have implemented these spin-dependent forces within the Cornell potential model [$\chi_{c0(2)}$ acquires a repulsive (attractive) $\frac{1}{r^3}$ potential, respectively], and found that the curvatures of the radial wave functions of χ_{c0} and χ_{c2} are changed towards the opposite direction such that $\Omega < 1$. Therefore, the discrepancy between (20) and the BESIII measurement of \mathcal{R} even further deteriorates!

To closely examine the impact of NNLO corrections, we can also extract the nonperturbative factors $\overline{R'_{\chi_{c0,2}}}(\mu_\Lambda)$ from the measured two-photon widths of $\chi_{c0,2}$ in (1). In Table I we tabulated these fitted parameters at various levels of accuracy in α_s . Although the NNLO corrections to $\chi_{c0} \rightarrow \gamma\gamma$ are sizable, one is still able to obtain a reasonable value for the matrix element; however, for the $\chi_{c2} \rightarrow \gamma\gamma$, both NLO and NNLO corrections are negative yet substantial, such that the partial width turns negative in some parameter space, and we refrain from listing the fitted value of $\overline{R'_{\chi_{c2}}}$ in Table I.

In Fig. 2, we show the values of $|\overline{R'_{\chi_{c0,2}}}(\mu_\Lambda)|^2$ fitted to account for the BESIII data following the NNLO for-

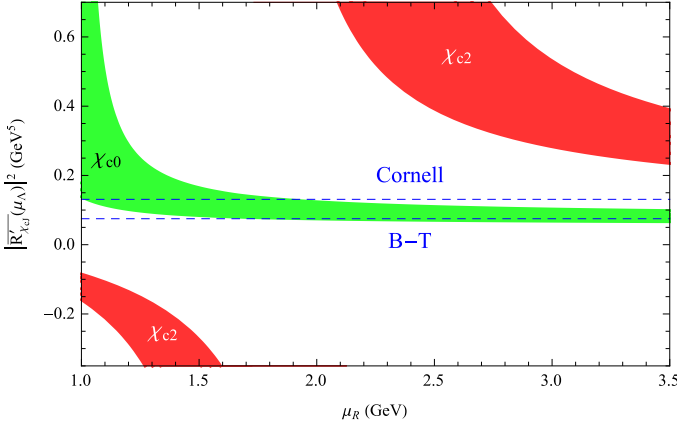


FIG. 2: The dependence of $|\overline{R'_{\chi_{cJ}}}(\mu_\Lambda)|^2$, which are fitted from the BESIII data using the NNLO formula, as a function of μ_R . The blue and green bands are obtained by varying μ_Λ from 1 GeV to m , and the two horizontal lines correspond to the respective values given by B-T and Cornell potential models [42].

mula, as a function of μ_R . For $\chi_{c0} \rightarrow \gamma\gamma$, within reasonable choice of μ_R and μ_Λ , the fitted $|\overline{R'_{\chi_{c0}}}|^2$ agrees with those predicted from the famous Cornell and Buchmüller-Tye (B-T) potential models [42]. However, for small μ_R , the fitted $|\overline{R'_{\chi_{c2}}}|^2$ becomes negative, hence unphysical; for large μ_R , $|\overline{R'_{\chi_{c2}}}|^2 > |\overline{R'_{\chi_{c0}}}|^2$ so that $\Omega > 1$, in contradiction to what is implied by the spin-dependent force. While the NNLO corrections to $\chi_{c0} \rightarrow \gamma\gamma$ are under theoretical control, it appears rather challenging to account for the $\chi_{c2} \rightarrow \gamma\gamma$ data from our results.

It is straightforward to adapt (17) to analyze P -wave bottomonia decays to two photons, by taking $n_L = 4$. The NLO perturbative predictions are

$$\mathcal{R}^b = (0.169_{-0.073}^{+0.015}) \Omega^b, \quad f_{0/2}^b = 0, \quad (21)$$

where Ω^b is the bottomonium counterpart of (18). After incorporating the NNLO corrections, we then predict

$$\mathcal{R}^b = (0.126_{-0.144}^{+0.025}) \Omega, \quad f_{0/2}^b = 0.0004_{-0.0001}^{+0.0014}, \quad (22)$$

where the central values are obtained by setting $\mu_\Lambda = \frac{m_b}{2}$ and $\mu_R = m_b$. The uncertainty is estimated by varying μ_Λ, μ_R in the range $1 \text{ GeV} < \mu_\Lambda < m_b$ and $1 \text{ GeV} < \mu_R < 2m_b$. Notably, the convergence of perturbative expansion for $\chi_{bJ} \rightarrow \gamma\gamma$ has been considerably improved with respect to χ_{cJ} decay, and we also expect here the HQSS-violation has smaller impact.

To summarize, in this work we have computed, for the first time, the complete order- α_s^2 corrections to $\chi_{c,b} \rightarrow \gamma\gamma$ in NRQCD framework, deducing the corresponding SDCs for each helicity amplitude. The NNLO corrections to $\chi_{c0,2} \rightarrow \gamma\gamma$ are found to be substantial, and we find it rather difficult to account for the ratio of their decay rates recently measured by BESIII. This discrepancy

even deteriorates after incorporating the spin-dependent inter-quark interaction. To resolve this puzzle, it is worth computing higher-order radiative corrections, as well as including the relativistic corrections. However, our poor knowledge of the higher-order P -wave NRQCD matrix elements renders a sharp order- v^2 prediction unrealistic [43, 44]. In contrast, we believe our $\mathcal{O}(\alpha_s^2)$ predictions to $\chi_{b0,2} \rightarrow \gamma\gamma$ are trustworthy. Hopefully, the forthcoming Belle II experiments, and the next-generation high-energy colliders, will have a bright prospect to measure these two-photon decay channels, thereby test our predictions.

Acknowledgment. We thank Estia Eichten for enlightening discussion on the spin-dependent inter-quark force. W.-L. S. is supported by the National Natural Science Foundation of China under Grant No. 11447031, and by the Open Project Program of State Key Laboratory of Theoretical Physics under Grant No. Y4KF081CJ1, and also by the Fundamental Research Funds for the Central Universities under Grant No. SWU114003, No. XDJK2016C067. The work of F. F. is supported by the National Natural Science Foundation of China under Grant No. 11505285, and by the Fundamental Research Funds for the Central Universities. The work of Y. J. and S.-R. L. is supported in part by the National Natural Science Foundation of China under Grants No. 11475188, No. 11261130311 (CRC110 by DGF and NSFC), by the IHEP Innovation Grant under contract number Y4545170Y2, and by the State Key Lab for Electronics and Particle Detectors.

-
- [1] T. Appelquist and H. D. Politzer, Phys. Rev. Lett. **34**, 43 (1975).
 - [2] A. De Rujula and S. L. Glashow, Phys. Rev. Lett. **34**, 46 (1975).
 - [3] W. Kwong, P. B. Mackenzie, R. Rosenfeld and J. L. Rosner, Phys. Rev. D **37**, 3210 (1988).
 - [4] M. B. Voloshin, Prog. Part. Nucl. Phys. **61**, 455 (2008) [arXiv:0711.4556 [hep-ph]].
 - [5] Z. P. Li, F. E. Close and T. Barnes, Phys. Rev. D **43**, 2161 (1991).
 - [6] S. N. Gupta, J. M. Johnson and W. W. Repko, Phys. Rev. D **54**, 2075 (1996) [hep-ph/9606349].
 - [7] S. Godfrey and N. Isgur, Phys. Rev. D **32**, 189 (1985).
 - [8] C. R. Munz, Nucl. Phys. A **609**, 364 (1996) [hep-ph/9601206].
 - [9] D. Ebert, R. N. Faustov and V. O. Galkin, Mod. Phys. Lett. A **18**, 601 (2003) [hep-ph/0302044].
 - [10] H. W. Huang, C. F. Qiao and K. T. Chao, Phys. Rev. D **54**, 2123 (1996) [hep-ph/9601380].
 - [11] G. T. Bodwin, E. Braaten and G. P. Lepage, Phys. Rev. D **51**, 1125 (1995) [Phys. Rev. D **55**, 5853 (1997)] [hep-ph/9407339].
 - [12] A. Petrelli, M. Cacciari, M. Greco, F. Maltoni and M. L. Mangano, Nucl. Phys. B **514**, 245 (1998) [hep-ph/9707223].

- [13] J. J. Dudek and R. G. Edwards, Phys. Rev. Lett. **97**, 172001 (2006) [hep-ph/0607140].
- [14] K. M. Ecklund *et al.* [CLEO Collaboration], Phys. Rev. D **78**, 091501 (2008) [arXiv:0803.2869 [hep-ex]].
- [15] M. Ablikim *et al.* [BESIII Collaboration], Phys. Rev. D **85**, 112008 (2012) [arXiv:1205.4284 [hep-ex]].
- [16] R. Barbieri, R. Gatto and R. Kogerler, Phys. Lett. B **60**, 183 (1976).
- [17] R. Barbieri, M. Caffo, R. Gatto and E. Remiddi, Phys. Lett. B **95**, 93 (1980).
- [18] R. Barbieri, M. Caffo, R. Gatto and E. Remiddi, Nucl. Phys. B **192**, 61 (1981).
- [19] A. Czarnecki and K. Melnikov, Phys. Rev. Lett. **80** (1998) 2531 [hep-ph/9712222].
- [20] M. Beneke, A. Signer and V. A. Smirnov, Phys. Rev. Lett. **80** (1998) 2535 [hep-ph/9712302].
- [21] A. Czarnecki and K. Melnikov, Phys. Lett. B **519** (2001) 212 [hep-ph/0109054].
- [22] F. Feng, Y. Jia and W. L. Sang, arXiv:1505.02665 [hep-ph].
- [23] A. I. Onishchenko and O. L. Veretin, Eur. Phys. J. C **50**, 801 (2007) [hep-ph/0302132].
- [24] L. B. Chen and C. F. Qiao, arXiv:1503.05122 [hep-ph].
- [25] T. Hahn, Comput. Phys. Commun. **140**, 418 (2001) [hep-ph/0012260].
- [26] R. Mertig, M. Bohm and A. Denner, Comput. Phys. Commun. **64**, 345 (1991).
- [27] F. Feng and R. Mertig, arXiv:1212.3522.
- [28] F. Feng, Comput. Phys. Commun. **183**, 2158 (2012) [arXiv:1204.2314 [hep-ph]].
- [29] A. V. Smirnov, Comput. Phys. Commun. **189**, 182 (2014) [arXiv:1408.2372 [hep-ph]].
- [30] V. A. Smirnov, *Analytic tools for Feynman integrals*, Springer Tracts Mod. Phys. **250**, 1 (2012).
- [31] J. Gluza, K. Kajda and T. Riemann, Comput. Phys. Commun. **177**, 879 (2007) [arXiv:0704.2423 [hep-ph]].
- [32] M. Czakon, Comput. Phys. Commun. **175**, 559 (2006) [hep-ph/0511200].
- [33] A. V. Smirnov, Comput. Phys. Commun. **185**, 2090 (2014) [arXiv:1312.3186 [hep-ph]].
- [34] R. Cools and A. Haegemans, ACM Trans. Math. Softw. **29** (2003), no. 3 287 C296.
- [35] D. J. Broadhurst, N. Gray and K. Schilcher, Z. Phys. C **52**, 111 (1991).
- [36] K. Melnikov and T. van Ritbergen, Nucl. Phys. B **591**, 515 (2000) [hep-ph/0005131].
- [37] A. H. Hoang and P. Ruiz-Femenia, Phys. Rev. D **74**, 114016 (2006) [hep-ph/0609151].
- [38] J. H. Kuhn, J. Kaplan and E. G. O. Safiani, Nucl. Phys. B **157**, 125 (1979).
- [39] Y. Kiyo, A. Pineda and A. Signer, Nucl. Phys. B **841**, 231 (2010) [arXiv:1006.2685 [hep-ph]].
- [40] K. G. Chetyrkin, J. H. Kuhn and M. Steinhauser, Comput. Phys. Commun. **133**, 43 (2000) [hep-ph/0004189].
- [41] N. Brambilla and A. Vairo, Phys. Rev. D **71**, 034020 (2005) [hep-ph/0411156].
- [42] E. J. Eichten and C. Quigg, Phys. Rev. D **52**, 1726 (1995) [hep-ph/9503356].
- [43] J. P. Ma and Q. Wang, Phys. Lett. B **537**, 233 (2002) [hep-ph/0203082].
- [44] N. Brambilla, E. Mereghetti and A. Vairo, JHEP **0608**, 039 (2006) [Erratum-ibid. **1104**, 058 (2011)] [hep-ph/0604190].